Journal of Magnetic Resonance 208 (2011) 270–278

Contents lists available at ScienceDirect

Journal of Magnetic Resonance

journal homepage: www.elsevier.com/locate/jmr

J-modulation effects in DOSY experiments and their suppression: The Oneshot45 experiment

Adolfo Botana, Juan A. Aguilar, Mathias Nilsson *, Gareth A. Morris

School of Chemistry, University of Manchester, Manchester M13 9PL, UK

ARTICLE INFO

Article history:
Received 1 October 2010
Revised 17 November 2010
Available online 21 November 2010

Keywords:
NMR
^{1}H DOSY
Diffusion-ordered spectroscopy
Diffusion
Oneshot
J-modulation
Phase distortions
Purging pulse

ABSTRACT

Diffusion-ordered spectroscopy (DOSY) is a powerful NMR method for identifying compounds in mixtures. DOSY experiments are very demanding of spectral quality; even small deviations from expected behaviour in NMR signals can cause significant distortions in the diffusion domain. This is a particular problem when signals overlap, so it is very important to be able to acquire clean data with as little overlap as possible. DOSY experiments all suffer to a greater or lesser extent from multiplet phase distortions caused by *J*-modulation, requiring a trade-off between such distortions and gradient pulse width. Multiplet distortions increase spectral overlap and may cause unexpected and misleading apparent diffusion coefficients in DOSY spectra. These effects are described here and a simple and effective remedy, the addition of a 45° purging pulse immediately before the onset of acquisition to remove the unwanted anti-phase terms, is demonstrated. As well as affording significantly cleaner results, the new method allows much longer diffusion-encoding pulses to be used without problems from *J*-modulation, and hence greatly increases the range of molecular sizes that can be studied for coupled spin systems. The sensitivity loss is negligible and the added phase cycling is modest. The new method is illustrated for a widely-used general purpose DOSY pulse sequence, Oneshot.

© 2010 Elsevier Inc. All rights reserved.

1. Introduction

Diffusion-ordered spectroscopy (DOSY [1,2]), a widely used pulsed field gradient NMR technique, aims to separate the component spectra of mixtures by virtue of the different diffusion behaviour of the molecular species involved. In a DOSY experiment a series of pulsed field gradient spin or stimulated echo spectra is acquired with increasing pulsed field gradient strength, causing a signal attenuation ideally described by the equation

$$S = S_0\, e^{-D\gamma^2\delta^2G^2\Delta'} \quad (1)$$

where S is the signal amplitude, S_0 is the amplitude that would have resulted without diffusion, D is the diffusion coefficient, δ is the gradient pulse width, γ is the magnetogyric ratio, G is the gradient amplitude, and Δ' is the effective diffusion time. For diffusion encoding to be effected, pulsed field gradients have to be applied while magnetization is in the transverse plane, typically either in a spin echo or in a stimulated echo. In such echoes, the chemical shift is refocused but the scalar coupling is not, thus leading to a *J*-modulated spectrum for coupled spin systems [3]. *J*-modulated spectra have peaks with both absorption and dispersive components, the latter leading to increased spectral overlap because of the much slower decay with frequency offset of the dispersion mode. Pulsed field gradient stimulated echo (PFGSTE) sequences [4,5] are generally preferred to spin echo sequences in DOSY because the magnetization spends less time in the transverse plane, leading to less *J*-modulation (and also often to less signal loss through relaxation). The growing application of DOSY to samples containing large, slowly diffusing species such as micelles [6,7], hydrocarbon mixtures [8,9], proteins [10,11] and DNA [12] is increasing demands for strong diffusion encoding. Gradient coils are limited in the amplitude of the gradient that they can generate, so in order to obtain stronger diffusion encoding it is typically necessary to increase gradient pulse widths, resulting in greater *J*-modulation. The latter phenomenon is frequently the limiting factor in determining the limiting size of species for which useful measurements can be made.

The best diffusion resolution in DOSY is obtained when there is no spectral overlap (the High Resolution DOSY, HR-DOSY [13] case), since each resonance can safely be assumed to belong to a single species and fitted to a two-parameter monoexponential decay. As a consequence, a wide variety of experiments have been devised to minimize overlap either by simplifying spectra [14–18] or by spreading out resonances in more dimensions [19–22]. ^{1}H HR-DOSY is the most commonly used DOSY technique, because of the relatively simple experimental setup, data processing and interpretation, and because of the high signal-to-noise ratio and efficient diffusion encoding afforded by the high ^{1}H magnetogyric

* Corresponding author. Fax: +44 (0) 161 275 4598.
E-mail address: mathias.nilsson@manchester.ac.uk (M. Nilsson).

1090-7807/$ - see front matter © 2010 Elsevier Inc. All rights reserved.
doi:10.1016/j.jmr.2010.11.012

ratio. However, it is a rare luxury for HR-DOSY to be applied in systems where there is no signal overlap at all; in most practical applications some overlap is present, and is tolerated because the effect on the HR-DOSY spectrum is normally simple and predictable: where two positive signals with different diffusion coefficients D_1 and D_2 overlap, the result of monoexponential fitting is to yield a compromise diffusion coefficient intermediate between D_1 and D_2. However, in this investigation it is shown that *J*-modulation can complicate matters. We analyse how the apparent diffusion coefficient of a signal is altered when it is overlapped by negative signals (typically from dispersive components in *J*-modulated spectra), and propose a new method to suppress these dispersive components.

2. *J*-modulation and its effects in DOSY experiments

J-modulation is typically seen in homonuclear spin and stimulated echoes because the effect of the scalar coupling remains while the chemical shift is refocused. In the widely adopted product operator description of spin manipulation [23] the transverse magnetization of an AX system of two spins-½ I_1 and I_2 after a spin echo (90° – τ/2 – 180° – τ/2 –) can be represented by the following operators:

$$M_{xy} = \cos(\pi J_{12}\tau)\hat{I}_{1x} + \sin(\pi J_{12}\tau)2\hat{I}_{1y}\hat{I}_{2z} + \cos(\pi J_{12}\tau)\hat{I}_{2x} + \sin(\pi J_{12}\tau)2\hat{I}_{2y}\hat{I}_{1z} \quad (2)$$

The $\hat{I}_{1x}$ and $\hat{I}_{2x}$ terms represent in-phase magnetization, and are normally phased to absorption mode in the resultant spectrum. However, the anti-phase terms $\hat{I}_{1y}\hat{I}_{2z}$ and $\hat{I}_{1z}\hat{I}_{2y}$ that arise from *J*-modulation contribute dispersion mode components to the lineshape. The dispersion mode has positive and negative lobes, and as noted earlier has a much larger frequency footprint than the absorption mode, because the signal intensity decays only hyperbolically with frequency offset at large offsets.

The complications caused by *J*-modulation in HR-DOSY arise because of signal overlap, which is increased by the presence of dispersive signal components. Where two signals overlap, the signal decay fitted to a monoexponential function is actually biexponential:

$$S = S_1\,e^{-D_1\gamma^2\delta^2G^2\Delta'} + S_2\,e^{-D_2\gamma^2\delta^2G^2\Delta'} \quad (3)$$

where S_1 and S_2 are the amplitudes of the overlapping signals in the absence of diffusion and D_1 and D_2 are the diffusion coefficients. In the familiar case where both signals are positive, the monoexponential fit to Eq. (1) will lead to a fitted amplitude S_m and to an estimated apparent diffusion coefficient D_m that is intermediate between D_1 and D_2, as for example in the illustration of Fig. 1a. For similar D_1 and D_2 the effect on the quality of fit is very small [24], which makes it difficult to detect deviations from mono-exponentiality, but users of DOSY routinely allow for this effect of overlap when interpreting experimental HR-DOSY spectra.

The first complication caused by *J*-modulation is thus an increase in the number and extent of signal overlaps. The second complication is more subtle: where positive and negative signals overlap, the fitted diffusion coefficient D_m no longer lies between D_1 and D_2. For this case where S_1 and S_2 in Eq. (3) have opposite sign, assuming that $|S_1| > |S_2|$ and that $S_2 < 0$, there are three cases that can be distinguished (see Appendix A):

Case 1: $D_1 > D_2$ and $S_m > 0$: the fitted D_m will be greater than both D_1 and D_2, as illustrated in Fig. 1b.

Case 2: $D_1 < D_2$ and $S_m > 0$: the fitted D_m will be lower than both D_1 and D_2, as illustrated in Fig. 1c.

Case 3: $D_1 > D_2$ and $S_m < 0$: the fitted D_m will be lower than both D_1 and D_2, as illustrated in Fig. 1d.

Case 3 typically leads to the fitting algorithm returning a large estimated relative error in D_m, which may cause a peak to be ignored (as not statistically significant) by programs for synthesising DOSY spectra.

While it might be expected that the presence of a biexponential decay should readily be apparent from an increase in the error in D_m estimated by the fitting algorithm, in practice such increases are often small, and far from diagnostic, as in Fig. 1a and c. Both missing signals and signals with unexpected apparent diffusion coefficients can easily lead to a misjudgement of the number and nature of species in a sample when DOSY spectra containing overlapping signals are interpreted. The presence of negative signals from the dispersion mode tails of *J*-modulated multiplets can also complicate multivariate analysis of diffusion-weighted data, since such analysis often applies non-negativity constraints [25–28].

3. Suppression of *J*-modulation effects

J-evolution is unavoidable in DOSY experiments, as magnetization needs to be in the transverse plane during diffusion encoding, typically in a spin or stimulated echo. For homonuclear couplings, unlike heteronuclear *J* couplings which can be refocused by applying a 180° pulse to the passive coupled nuclei, there is no general solution that allows the refocusing of scalar couplings (with the exception of pure shift experiments, *vide infra*), although partial solutions have been reported. Takegoshi et al. [29] and van Zijl et al. [30] reported that a double spin echo with a 90° pulse orthogonal to the first pulse at the time of the first echo can be used to refocus *J*-evolution for a two-spin system, but that this refocusing is incomplete for higher order spin systems; this approach has been recently implemented for PFG spin echo experiments [31]. The oscillating-gradient spin echo [32] has been used to obtain pure absorption mode spectra for systems with specific coupling constants. Homonuclear decoupling during spin evolution in principle avoids evolution into anti-phase terms [33], but in practice cannot decouple all spins at once. Homonuclear *J*-evolution can be refocused by manipulating spins using combined frequency and spatially selective pulses in so-called pure shift experiments [14,15], but these incur significant sensitivity penalties. In addition, none of the above methods can reliably suppress *J*-modulation in strongly coupled spin systems.

Given the difficulty of achieving a complete refocusing of homonuclear scalar couplings, other work has focused on methods for purging the unwanted magnetization, but all the methods proposed to date suffer from significant limitations and complications. Torres et al. [34] have recently evaluated the performance of three such purging elements in PFG spin and stimulated echo sequences. A spin-lock, or trim, pulse before acquisition removes anti-phase magnetization without affecting the in-phase magnetization [4]. However, the sample is not field-frequency locked while the pulse is applied, which may lead to a deterioration in lineshape, and the radiofrequency power deposited causes sample heating [35,36], which can be highly detrimental to DOSY experiments if it results in convection. A Longitudinal Eddy Delay (LED) or *z*-filter element [37], which includes a homospoil or gradient pulse, removes anti-phase magnetization to some extent [38,39]. The first 90° pulse converts in-phase magnetization into longitudinal, and anti-phase into multiple and zero quantum coherences. The gradient dephases multiple quantum coherences, but not zero quantum coherences. The second 90° pulse converts longitudinal magnetization back into in-phase and zero quantum coherences into anti-phase magnetization. The last alternative evaluated is the chirp-based *z*-filter,

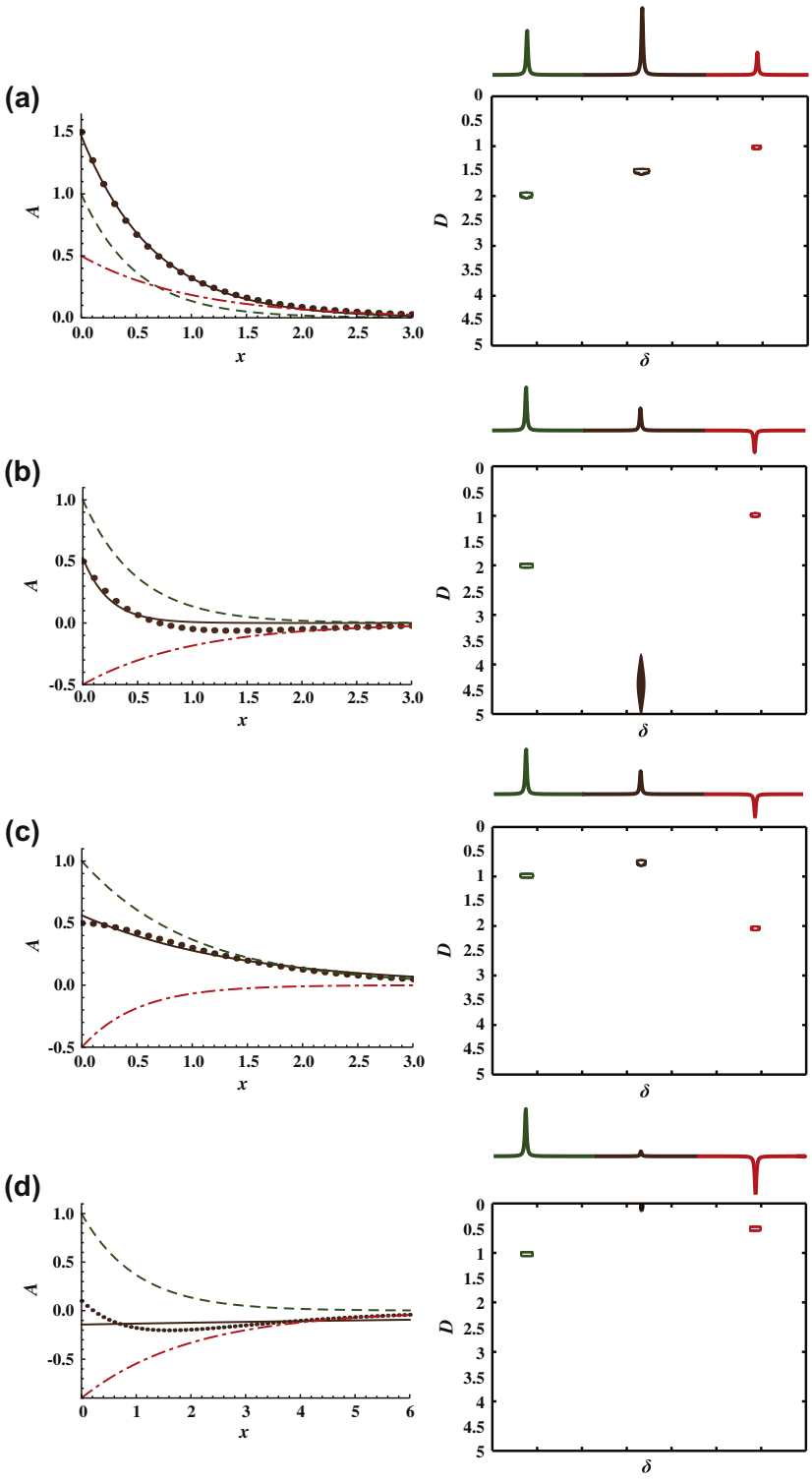

Fig. 1. Result of monoexponential fitting of a sampled biexponential function resulting from the addition of two exponential functions $A = S\,e^{-Dx}$ with amplitudes S_1 and S_2 and diffusion coefficients D_1 and D_2. In each case the D_m obtained depends on the exact choice of points to sample. Green dashed and red dot-dashed lines show the variation of amplitude A evolution with x for two exponentials with decay constants D_1 (green) and D_2 (red). Brown dots show sampled points from the sum of the two exponentials and the continuous brown line a monoexponential fitted to the sampled points. On the right side is the simulated DOSY plot that would be obtained with two chemically shifted signals from each of two different species, with the two inner peaks overlapping exactly. (a) Monoexponential fitting of the sum of two positive exponentials with amplitudes $S_1 = 1$ and $S_2 = 0.5$ and decay constants $D_1 = 2$ and $D_2 = 1$ yields an apparent diffusion coefficient $D_m = 1.52$, between D_1 and D_2. (b) Monoexponential fitting of the sum of exponentials with amplitudes $S_1 = 1$ and $S_2 = -0.5$ and decay constants $D_1 = 2$ and $D_2 = 1$ yields an apparent diffusion coefficient $D_m = 4.18$, greater than either D_1 or D_2 (case 1 in text). (c) Monoexponential fitting of the sum of exponentials with amplitudes $S_1 = 1$ and $S_2 = -0.5$ and decay constants $D_1 = 1$ and $D_2 = 2$ yields an apparent diffusion coefficient $D_m = 0.70$, less than either D_1 or D_2 (case 2 in text). (d) Monoexponential fitting of the sum of exponentials with amplitudes $S_1 = 1$ and $S_2 = -0.9$ and decay constants $D_1 = 1$ and $D_2 = 0.5$ yields an apparent diffusion coefficient $D_m = 0.07$, less than either D_1 or D_2 (case 3 in text) (For interpretation of the references to color in this figure legend, the reader is referred to the web version of this article.).

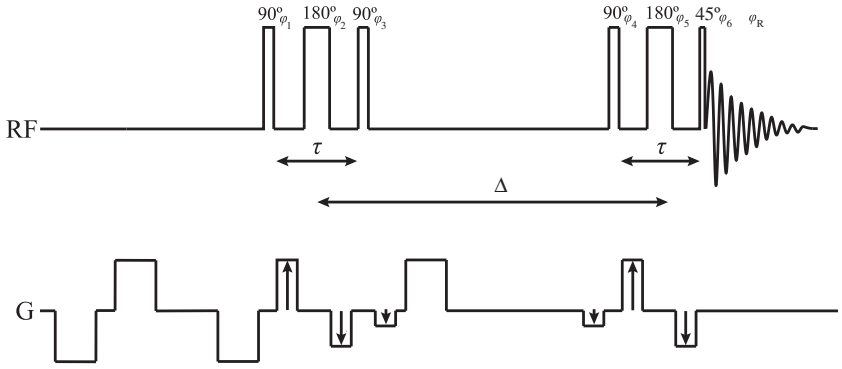

Fig. 2. Oneshot45 pulse sequence, which consists of Oneshot plus a 45° pulse orthogonal to the preceding 90° pulse.

in which a chirp pulse synchronous with a gradient [40] is included in the LED element. This combination dephases zero quantum coherences, thus leaving only in-phase magnetization. All these three elements lose sensitivity due to relaxation losses, and the latter two require extensive phase cycling for clean results.

3.1. Oneshot45

In this investigation we propose an alternative solution, the addition of a final 45° pulse orthogonal to the preceding 90° pulse. This idea has been used previously for obtaining pure phase homonuclear and heteronuclear 2D spectra, either in the same form [41] or as a pulse pair [42]. It efficiently removes anti-phase magnetization without the drawbacks of previous methods. It is worth noting here that the product operator description of Eq. (2) for transverse magnetization after a spin echo contains in-phase and anti-phase magnetizations with orthogonal phases, and that these can therefore be manipulated independently by radiofrequency pulses; the same is true for a stimulated echo. If a 45° pulse is applied along the *x*-axis immediately after the modulated echo, the in-phase magnetization is unaffected but the anti-phase terms are changed:

$$\begin{aligned}&\sin(\pi J_{12}\tau)2\hat{I}_{1y}\hat{I}_{2z} + \sin(\pi J_{12}\tau)2\hat{I}_{2y}\hat{I}_{1z} \overset{\pi/4(\hat{I}_{1x}+\hat{I}_{2x})}{\rightarrow} \cos(\pi/4)\\ &\quad\times \sin(\pi J_{12}\tau)2\hat{I}_{1y}\hat{I}_{2z} - \sin(\pi/4)\sin(\pi J_{12}\tau)2\hat{I}_{1z}\hat{I}_{2y} + \cos(\pi/4)\\ &\quad\times \sin(\pi J_{12}\tau)2\hat{I}_{2y}\hat{I}_{1z} - \sin(\pi/4)\sin(\pi J_{12}\tau)2\hat{I}_{2z}\hat{I}_{1y}\end{aligned}$$

Since $\cos(\pi/4) = \sin(\pi/4)$, these terms cancel and the unwanted anti-phase magnetization is removed. The analysis for higher order spin systems is analogous (see Appendix B). All bilinear terms (those of the form $2\hat{I}_{iy}\hat{I}_{jz}$, with *i* and *j* being the coupled spins) cancel out, and half of the coherence from higher order terms is transformed into undetectable multiple quantum coherences. The 45° purging pulse thus allows, in theory, the complete removal of all anti-phase magnetization from AX systems and, for short echo times, most anti-phase magnetization for more complex spin systems.

The additional pulse requires only a two-step phase cycle for clean results, so the increase in minimum experiment time is modest. The new purging pulse is demonstrated here using the Oneshot [5] pulse sequence, routinely used in DOSY, that provides good spectral quality with a minimum of phase cycling. This combination of the Oneshot sequence and the 45° purging pulse, called Oneshot45, is depicted in Fig. 2, and the full phase cycling given in Table 1; the minimum phase cycle for clean results is just two transients. The sequence contains two spin echoes, but any anti-phase magnetization generated in the first spin echo is converted into multiple quantum coherences by the second 90° pulse, and these coherences are not converted back into detectable magnetization. The phase shifts introduced by *J*-modulation are thus determined solely by the duration τ of the second echo.

4. Experimental

Data were acquired for two mixtures, one of 1-propanol (250 mM) and 2-pentanol (75 mM) in deuterated dimethyl sulfoxide (DMSO-d_6) with 27 mM TSP (sodium 3-(trimethylsilyl)-propionate-2,2,3,3-d_4) as a reference, and the other camphene (20 mM), geraniol (23 mM) and quinine (19 mM), dissolved in methanol-d_4 with TMS (tetramethylsilane) as a reference. Measurements were carried out non-spinning on a Varian VNMRS 500 spectrometer in an air-conditioned room at approximately 20 °C, with probe temperature regulation set at 25 °C and with a passive air preconditioning system used to minimize temperature variations [43].

A series of experiments were carried out with Oneshot and Oneshot45 to evaluate the effects of *J*-modulation on the corresponding DOSY spectra. Data sets for the mixture of 1-propanol and 2-pentanol were acquired in 5 min with 10 gradient amplitudes ranging from 10 to 30 G cm^{-1} in equal steps of gradient squared, using four transients, 8192 complex data points, a total diffusion-encoding gradient duration of 1.8 ms, and a diffusion time of 0.2 s. The spin echo time was varied from 2.8 to 13.8 ms to map out *J*-modulation effects for a range of echo times. Data for the mixture of quinine, camphene and geraniol were acquired in 7 min with 8 gradient amplitudes ranging from 10 to 30 G cm^{-1} in equal steps of gradient squared using four transients, 16,384 complex data points, a total diffusion-encoding gradient duration of 3.6 ms, an echo time of 19.6 ms and a diffusion time of 0.1 s. The long echo delays used here are to illustrate the effects of long duration of gradient pulses, required for the analysis of large molecules, as for example in the case of a recent paper where 8.5 ms gradient pulses were used for a study of dextran polymers [44]. Nevertheless, problems can arise even for relatively modest echo times and small molecules if large and small signals are close together, as will be shown.

5. Results and discussion

The Oneshot DOSY spectrum for the mixture of 1-propanol and 2-pentanol using an echo time of 13.8 ms shows peaks (Fig. 3a) for the two methyl resonances with three different apparent diffusion coefficients. The outer peak of the 2-pentanol methyl triplet, at 0.90 ppm (marked with a circle in Figs. 3a and 4a), overlaps with the 1-propanol methyl triplet, and has an apparent diffusion coefficient which is lower than that of the two alcohols. This arises because the small 2-pentanol signal sits on the dispersive tail of the large 1-propanol signal, and is a practical example of the situation

Table 1
Phase cycling for Oneshot45. Phases are notated as multiples of 90° (0 = 0°, 1 = 90°, 2 = 180°, 3 = 270°), with subscripts denoting repetition; the minimum phase cycle is two transients.

φ_1	$0_4 1_4 + 02$
φ_2	$0_{128} 2_{128}$
φ_3	$0_{32} 2_{32}$
φ_4	$0_2 2_2 + 0_8 1_8 2_8 3_8$
φ_5	$0_{64} 1_{64} + 0_{16} 2_{16}$
φ_6	$\varphi_1 - 2\varphi_2 + \varphi_3 - \varphi_4 + 2\varphi_5 + 1 + 0_4 2_4 + 02$
φ_R	$\varphi_1 - 2\varphi_2 + \varphi_3 - \varphi_4 + 2\varphi_5$

illustrated in Fig. 1c. In cases like this it would be easy to draw the erroneous conclusion that there is a high molecular weight species in the mixture. In contrast, Figs. 3b and 4b show data from the same sample acquired using the Oneshot45 sequence. In the DOSY spectrum (Fig. 3b) peaks in the diffusion dimension all appear at the expected positions, and from the 1D NMR spectrum in Fig. 4b it is clear that almost all of the problematic *J*-modulation has been successfully purged.

With these long echo times (outside the range normally used for DOSY experiments on small molecules, but typical of those needed to measure low diffusion coefficients with limited peak gradient amplitude), the spectra obtained with Oneshot45 (Figs. 3b and 4b) are largely unaffected by *J*-modulation. Fig. 5 shows the apparent diffusion coefficient as a function of echo time for well-resolved and for overlapping (0.90 ppm; highlighted in Figs. 3 and 4) peaks, for data measured using the Oneshot and Oneshot45 sequences. As expected, *J*-evolution has no effect on apparent diffusion coefficient for the resolved signals, but the effects of signal overlap are clearly noticeable for data acquired with the standard Oneshot sequence at echo times as low as 4 ms; Oneshot45 suppresses these undesired effects effectively even at an echo time of 14 ms.

The presence of some distortion even at echo times as low as 4 ms shows that problems with *J*-modulation in DOSY are not confined to high molecular mass samples, for which long echo times are needed. The impact of *J*-modulation depends both on the extent of modulation and on the relative intensities of the overlapping signals: a small phase error in a strong signal will cause a big proportionate shift in the intensity of a smaller signal sitting on its dispersion mode tail.

The mixture of quinine, geraniol and camphene was used to assess the performance of the two sequences with a more complex sample. In both Oneshot and Oneshot45 the severe overlap of small signals between 1 and 2 ppm makes it difficult to resolve the signals with standard HR-DOSY [13,28], but the rest of the spectrum appears to be resolved. However, *J*-modulation again is the cause of misleading results. The small doublet at 2.6 ppm appears to belong to geraniol as the apparent diffusion coefficient is consistent with that of other geraniol signals (Fig. 6a); in fact, a positive dispersive

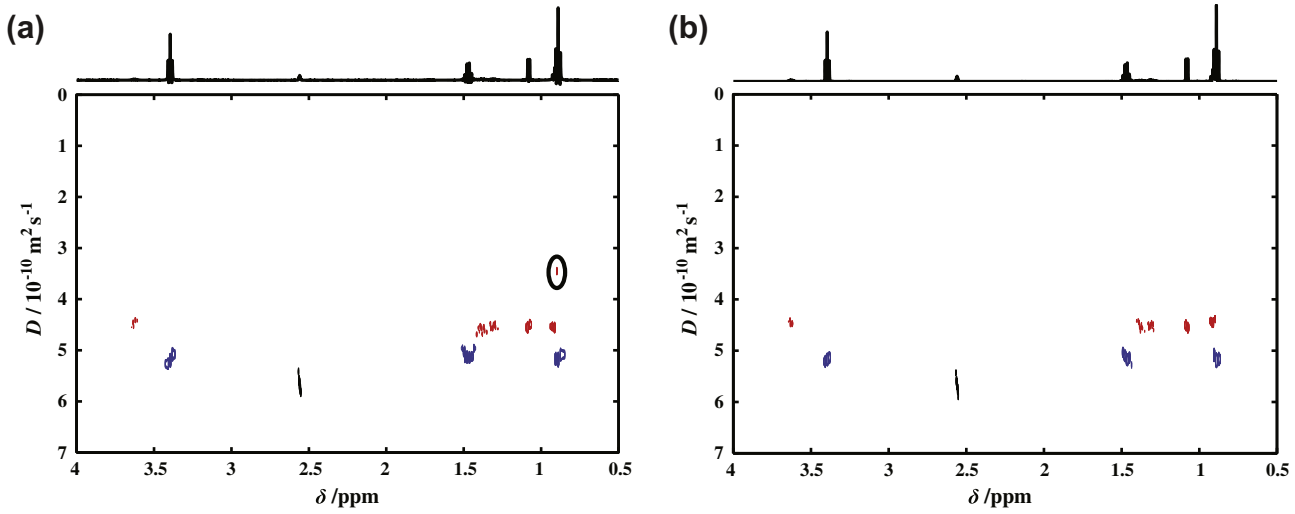

Fig. 3. (a) Oneshot and (b) Oneshot45 DOSY spectra of 1-propanol (blue) and 2-pentanol (red) with an echo time of 13.8 ms. The signal highlighted belongs to the 2-pentanol but has an apparent diffusion coefficient that is outside the range spanned by the two components (For interpretation of the references to color in this figure legend, the reader is referred to the web version of this article.).

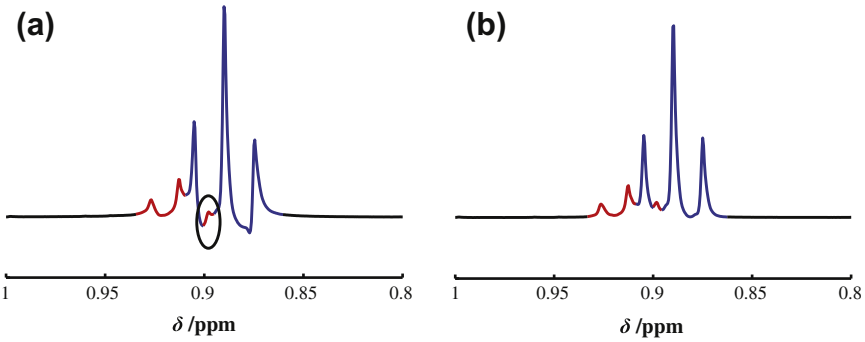

Fig. 4. Detail of the spectrum (a) obtained with Oneshot compared with the spectrum (b) obtained with Oneshot45 for the mixture of 1-propanol and 2-pentanol with an echo time of 13.8 ms. The peak amplitude of the signal highlighted is severely distorted by the dispersive negative tail of a 1-propanol peak, causing a misleading apparent diffusion coefficient (Fig. 3).

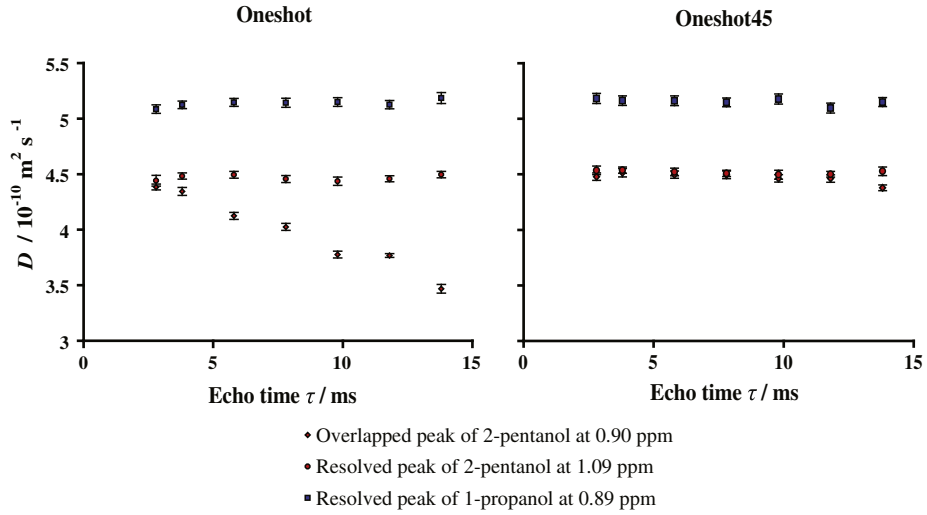

Fig. 5. Dependence of the apparent diffusion coefficients of selected diffusion peaks of the mixture of 1-propanol and 2-pentanol on echo time for (a) Oneshot and (b) Oneshot45. The apparent diffusion coefficient of the overlapped peak obtained with Oneshot diverges from the true diffusion coefficient with increasing echo time, but for the range of echo times shown Oneshot45 corrects this behaviour.

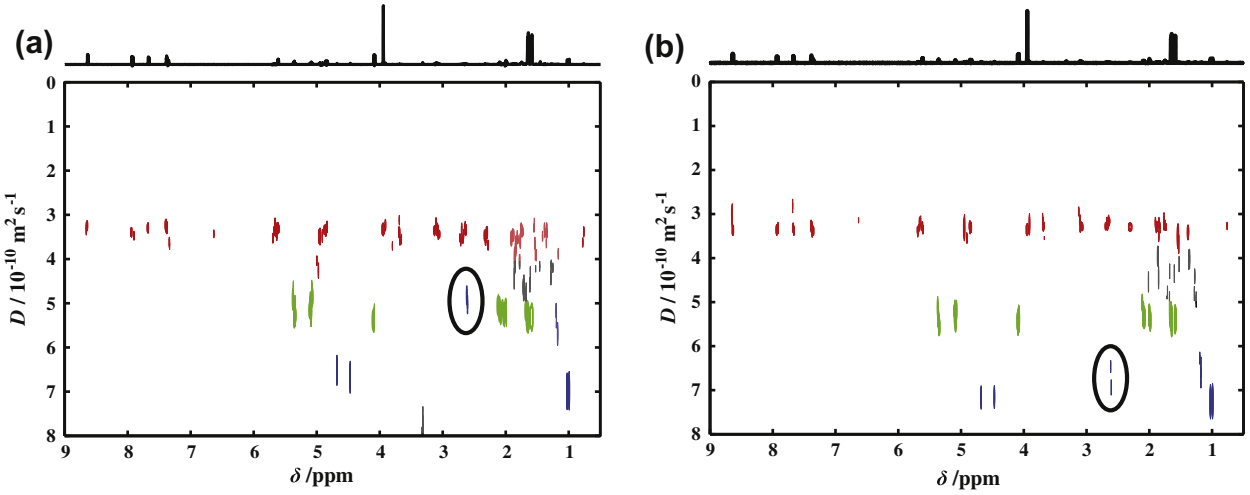

Fig. 6. (a) Oneshot and (b) Oneshot45 DOSY spectra of quinine (red), geraniol (green) and camphene (blue) with an echo time of 19.6 ms. In the Oneshot DOSY spectrum the highlighted doublet appears to belong to the geraniol spectrum, but actually originates from camphene as shown in the Oneshot45 spectrum (For interpretation of the references to color in this figure legend, the reader is referred to the web version of this article.).

tail from a quinine multiplet overlaps with this doublet, altering its apparent diffusion coefficient. Using the Oneshot45 sequence (Fig. 6b) the dispersive tail is suppressed and the apparent diffusion coefficient now comes out close to the correct value, showing that the doublet actually belongs to camphene.

6. Conclusions

In DOSY experiments, *J*-modulation can cause signal overlap, resulting in misleading apparent diffusion coefficients. When a peak overlaps with the positive tail of another peak belonging to a different species, the apparent diffusion coefficient calculated in HR-DOSY is intermediate between the diffusion coefficients of the two species. However, when the overlap is from a negative dispersive tail, as caused by *J*-modulation, the effect is counter-intuitive: the apparent diffusion coefficient is outside the range spanned by the two species. The magnetization responsible for this effect of *J*-modulation can be suppressed efficiently, even for relatively long echo times, by adding a 45° purging pulse immediately before acquisition. The Oneshot45 pulse sequence improves the reliability of DOSY data at no significant cost in sensitivity and with only a doubling of the (very short) minimum experiment time, making it ideal wherever rapid and reliable measurements are required, such as for the analysis of unstable mixtures [45] or reactions [46,47]. In addition, the suppression of distortions caused by *J*-modulation allows much longer gradient-encoding pulses to be used with coupled spin systems. Because of the square law dependence of the Stejskal–Tanner exponent on the gradient pulse width, this translates into an improvement of more than an order of magnitude in the limiting range of diffusion coefficients that can be studied with given hardware. Finally, the relatively small price to pay for the purging of unwanted magnetization also makes Oneshot45 a good candidate for a general purpose DOSY pulse sequence.

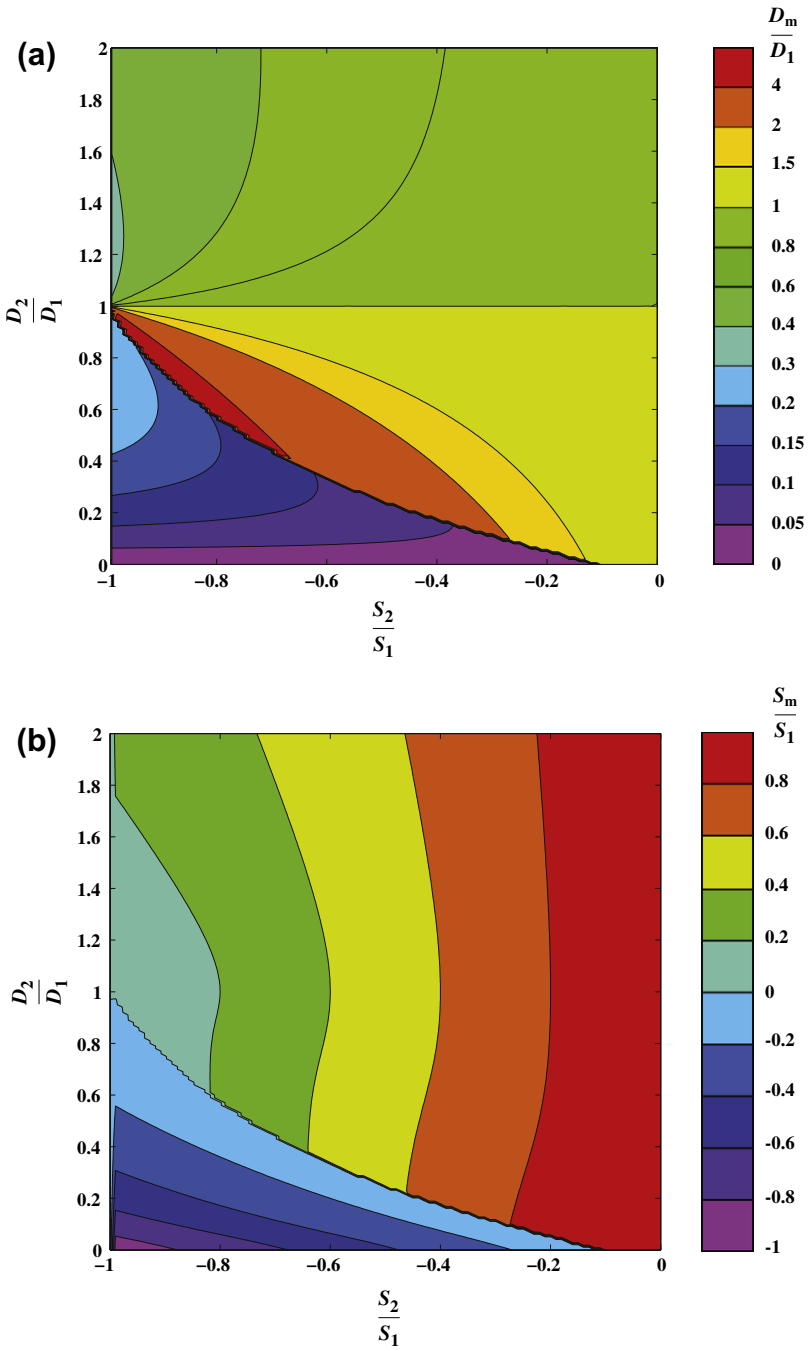

Fig. A1. Contour plots, as a function of the ratios S_2/S_1 and D_2/D_1 of relative amplitudes and decay constants of the components of a biexponential function, of (a) the best fit relative monoexponential rate constant D_m/D_1 and (b) the best fit relative monoexponential amplitude S_m/S_1.

Acknowledgment

This work was supported by the Engineering and Physical Sciences Research Council (Grant numbers EP/D05592X, EP/E05899X/1, and EP/E057888/1).

Appendix A

The existence and scope of the different cases for monoexponential least squares fitting of a biexponential curve can be demonstrated analytically. Consider the general biexponential function

$$S = S_1 e^{-D_1 x} + S_2 e^{-D_2 x} \tag{A1}$$

The variance between this and the monoexponential fit function

$$S = S_m e^{-D_m x} \tag{A2}$$

is given by

$$\begin{aligned}\chi^2 &= \int_0^\infty (S_1 e^{-D_1 x} + S_2 e^{-D_2 x} - S_m e^{-D_m x})^2 dx \\ &= \tfrac{1}{2}\left(\tfrac{S_1^2}{D_1} + \tfrac{S_2^2}{D_2} + \tfrac{S_m^2}{D_m} + \tfrac{4S_1S_2}{D_1+D_2} - \tfrac{4S_1S_m}{D_1+D_m} - \tfrac{4S_2S_m}{D_2+D_m}\right)\end{aligned} \tag{A3}$$

The turning points in χ^2 can be found by solving the simultaneous equations

$$\begin{aligned}\frac{d\chi^2}{dS_m} &= 0 = \frac{S_m}{D_m} - \frac{2S_1}{D_1+D_m} - \frac{2S_2}{D_2+D_m}\\ \frac{d\chi^2}{dD_m} &= 0 = \frac{1}{2}\left[\frac{4S_1S_m}{(D_1+D_m)^2} + \frac{4S_2S_m}{(D_2+D_m)^2} - \frac{S_m^2}{D_m^2}\right]\end{aligned} \tag{A4}$$

yielding four roots.

Fig. A1 shows contour plots of the relative values D_m/D_1 and S_m/S_1 that minimize Eq. (A2) (for $|S_1| > |S_2|$). A clear discontinuity is seen in both plots running down from the degenerate case of equal amplitudes and diffusion coefficients towards the line $D_2/D_1 = 0$. On one side of the discontinuity the best fit D_m rises sharply as it is approached, on the other it falls to a low value, corresponding to a change between the best fit monoexponential being fast and positive to being slow and negative. The three cases identified in the text correspond to (1) the top halves of the two plots, where $D_m < D_1$, D_2 and $S_m > 0$; (2) the lower right hand parts of the plots, where $D_m > D_1$, D_2 and $S_m > 0$; and (3) the lower left hand parts of the plots, where $D_m < D_1$, D_2 and $S_m < 0$.

Appendix B

In a system with three spins $\hat{I}_1$, $\hat{I}_2$ and $\hat{I}_3$ where magnetization is initially longitudinal, the effect of the spin echo will be as described by the following product operator transformations. For spin $\hat{I}_1$:

$$\hat{I}_{1z} \xrightarrow{\pi/2(\hat{I}_{1y})} \hat{I}_{1x} \xrightarrow{2\pi J_{12}\tau \hat{I}_{1z}\hat{I}_{2z}} \cos(\pi J_{12}\tau)\hat{I}_{1x} + \sin(\pi J_{12}\tau)2\hat{I}_{1y}\hat{I}_{2z}$$

$$\begin{aligned}&\cos(\pi J_{12}\tau)\hat{I}_{1x} + \sin(\pi J_{12}\tau)2\hat{I}_{1y}\hat{I}_{2z} \xrightarrow{2\pi J_{13}\tau \hat{I}_{1z}\hat{I}_{3z}} \cos(\pi J_{12}\tau)\cos(\pi J_{13}\tau)\hat{I}_{1x}\\ &\quad + \cos(\pi J_{12}\tau)\sin(\pi J_{13}\tau)2\hat{I}_{1y}\hat{I}_{3z} + \sin(\pi J_{12}\tau)\cos(\pi J_{13}\tau)2\hat{I}_{1y}\hat{I}_{2z}\\ &\quad - \sin(\pi J_{12}\tau)\sin(\pi J_{13}\tau)4\hat{I}_{1x}\hat{I}_{2z}\hat{I}_{3z}\end{aligned}$$

The product operator transformations are analogous for spins $\hat{I}_{2x}$ and $\hat{I}_{3x}$. After the application of a 45° pulse the operators experience the following transformations:

$$\begin{aligned}&\cos(\pi J_{12}\tau)\cos(\pi J_{13}\tau)\hat{I}_{1x} \xrightarrow{\pi/4(\hat{I}_{1x}+\hat{I}_{2x}+\hat{I}_{3x})} \cos(\pi/4)\cos(\pi J_{12}\tau)\\ &\quad \times \cos(\pi J_{13}\tau)\hat{I}_{1x}\end{aligned}$$

$$\begin{aligned}&\cos(\pi J_{12}\tau)\sin(\pi J_{13}\tau)2\hat{I}_{1y}\hat{I}_{3z} \xrightarrow{\pi/4(\hat{I}_{1x}+\hat{I}_{2x}+\hat{I}_{3x})} \cos(\pi/4)\cos(\pi J_{12}\tau)\\ &\quad \times \sin(\pi J_{13}\tau)2\hat{I}_{1y}\hat{I}_{3z} - \sin(\pi/4)\cos(\pi J_{12}\tau)\sin(\pi J_{13}\tau)2\hat{I}_{1z}\hat{I}_{3y}\end{aligned}$$

$$\begin{aligned}&\sin(\pi J_{12}\tau)\cos(\pi J_{13}\tau)2\hat{I}_{1y}\hat{I}_{2z} \xrightarrow{\pi/4(\hat{I}_{1x}+\hat{I}_{2x}+\hat{I}_{3x})} \cos(\pi/4)\sin(\pi J_{12}\tau)\\ &\quad \times \cos(\pi J_{13}\tau)2\hat{I}_{1y}\hat{I}_{2z} - \sin(\pi/4)\sin(\pi J_{12}\tau)\cos(\pi J_{13}\tau)2\hat{I}_{1z}\hat{I}_{2y}\end{aligned}$$

$$\begin{aligned}&-\sin(\pi J_{12}\tau)\sin(\pi J_{13}\tau)4\hat{I}_{1x}\hat{I}_{2z}\hat{I}_{3z} \xrightarrow{\pi/4(\hat{I}_{1x}+\hat{I}_{2x}+\hat{I}_{3x})} -\cos(\pi/4)\sin(\pi J_{12}\tau)\\ &\quad \times \sin(\pi J_{13}\tau)4\hat{I}_{1x}\hat{I}_{2z}\hat{I}_{3z} - \sin(\pi/4)\sin(\pi J_{12}\tau)\sin(\pi J_{13}\tau)4\hat{I}_{1x}\hat{I}_{2y}\hat{I}_{3y}\end{aligned}$$

The in-phase terms are unaffected, the bilinear anti-phase terms are cancelled by the corresponding bilinear anti-phase terms of the other two spins, and the trilinear anti-phase terms are partially converted into unobservable multiple quantum coherences. The observable terms that survive are a thus a mixture of in-phase, and reduced trilinear anti-phase, magnetization. The amplitudes of the trilinear terms depend on the product of two sine functions of τ, and so are negligible for short echo times.

References

[1] C.S. Johnson, Diffusion ordered nuclear magnetic resonance spectroscopy: principles and applications, Prog. Nucl. Magn. Reson. Spectrosc. 34 (1999) 203–256.
[2] G.A. Morris, Diffusion-ordered spectroscopy, in: R.K. Harris, R.E. Wasylishen, (Eds.), Encyclopedia of Magnetic Resonance. Chichester, John Wiley, doi:10.1002/9780470034590.emrstm0119.pub2.
[3] J. Keeler, Understanding NMR Spectroscopy, John Wiley, Chichester, 2005.
[4] M.D. Pelta, H. Barjat, G.A. Morris, A.L. Davis, S.J. Hammond, Pulse sequences for high-resolution diffusion-ordered spectroscopy (HR-DOSY), Magn. Reson. Chem. 36 (1998) 706–714.
[5] M.D. Pelta, G.A. Morris, M.J. Stchedroff, S.J. Hammond, A one-shot sequence for high-resolution diffusion-ordered spectroscopy, Magn. Reson. Chem. (2002) S147–S152.
[6] D. Šmejkalová, A. Piccolo, Aggregation and disaggregation of humic supramolecular assemblies by NMR diffusion ordered spectroscopy (DOSY-NMR), Environ. Sci. Technol. 42 (2007) 699–706.
[7] P.S. Denkova, L. Van Lokeren, R. Willem, Mixed micelles of Triton X-100, sodium dodecyl dioxyethylene sulfate, and Synperonic L61 investigated by NOESY and diffusion ordered NMR spectroscopy, J. Phys. Chem. B 113 (2009) 6703–6709.
[8] G.S. Kapur, M. Findeisen, S. Berger, Analysis of hydrocarbon mixtures by diffusion-ordered NMR spectroscopy, Fuel 79 (2000) 1347–1351.
[9] E. Durand, M. Clemancey, A.-A. Quoineaud, J. Verstraete, D. Espinat, J.-M. Lancelin, ^{1}H diffusion-ordered spectroscopy (DOSY) nuclear magnetic resonance (NMR) as a powerful tool for the analysis of hydrocarbon mixtures and asphaltenes, Energy Fuels 22 (2008) 2604–2610.
[10] C. Pascal, F. Paté, V. Cheynier, M.-A. Delsuc, Study of the interactions between a proline-rich protein and a flavan-3-ol by NMR: residual structures in the natively unfolded protein provides anchorage points for the ligands, Biopolymers 91 (2009) 745–756.
[11] A. Martínez-Cruz Luis, J.A. Encinar, D. Kortazar, J. Prieto, J. Gómez, P. Fernández-Millán, M. Lucas, A. Arribas Egoitz, J.A. Fernández, M.L. Martínez-Chantar, J.M. Mato, J.L. Neira, The CBS domain protein MJ0729 of *Methanocaldococcus jannaschii* is a thermostable protein with a pH-dependent self-oligomerization, Biochemistry 48 (2009) 2760–2776.
[12] A. Ambrus, D. Yang, Diffusion-ordered nuclear magnetic resonance spectroscopy for analysis of DNA secondary structural elements, Anal. Biochem. 367 (2007) 56–67.
[13] H. Barjat, G.A. Morris, S. Smart, A.G. Swanson, S.C.R. Williams, High-resolution diffusion-ordered 2D spectroscopy (HR-DOSY) – a new tool for the analysis of complex mixtures, J. Magn. Reson., Ser B 108 (1995) 170–172.
[14] M. Nilsson, G.A. Morris, Pure shift proton DOSY: diffusion-ordered ^{1}H spectra without multiplet structure, Chem. Commun. (2007) 933–935.
[15] J.A. Aguilar, S. Faulkner, M. Nilsson, G.A. Morris, Pure Shift ^{1}H NMR: a resolution of the resolution problem?, Angew Chem. Int. Ed. 49 (2010) 3901–3903.
[16] J.C. Cobas, M. Martín-Pastor, A homodecoupled diffusion experiment for the analysis of complex mixtures by NMR, J. Magn. Reson. 171 (2004) 20–24.
[17] N. Giraud, M. Joos, J. Courtieu, D. Merlet, Application of a ^{1}H δ-resolved 2D NMR experiment to the visualization of enantiomers in chiral environment, using sample spatial encoding and selective echoes, Magn. Reson. Chem. 47 (2009) 300–306.
[18] G.A. Morris, J.A. Aguilar, R. Evans, S. Haiber, M. Nilsson, True chemical shift correlation maps: a TOCSY experiment with pure shifts in both dimensions, J. Am. Chem. Soc. 132 (2010) 12770–12772.
[19] D. Wu, A. Chen, J.C.S. Johnson, Three-dimensional diffusion-ordered NMR spectroscopy: the homonuclear COSY–DOSY experiment, J. Magn. Reson., Ser A 121 (1996) 88–91.
[20] H. Barjat, G.A. Morris, A.G. Swanson, A three-dimensional DOSY–HMQC experiment for the high-resolution analysis of complex mixtures, J. Magn. Reson. 131 (1998) 131–138.
[21] J.M. Newman, A. Jerschow, Improvements in complex mixture analysis by NMR: DQF-COSY iDOSY, Anal. Chem. 79 (2007) 2957–2960.
[22] M. Nilsson, A.M. Gil, I. Delgadillo, G.A. Morris, Improving pulse sequences for 3D diffusion-ordered NMR spectroscopy: 2DJ-IDOSY, Anal. Chem. 76 (2004) 5418–5422.
[23] O.W. Sørensen, G.W. Eich, M.H. Levitt, G. Bodenhausen, R.R. Ernst, Product operator formalism for the description of NMR pulse experiments, Prog. Nucl. Magn. Reson. Spectrosc. 16 (1984) 163–192.
[24] M. Nilsson, M.A. Connell, A.L. Davis, G.A. Morris, Biexponential fitting of diffusion-ordered NMR data: practicalities and limitations, Anal. Chem. 78 (2006) 3040–3045.
[25] L.C.M. Van Gorkom, T.M. Hancewicz, Analysis of DOSY and GPC-NMR experiments on polymers by multivariate curve resolution, J. Magn. Reson. 130 (1998) 125–130.
[26] W. Windig, B. Antalek, Direct exponential curve resolution algorithm (DECRA): a novel application of the generalized rank annihilation method for a single spectral mixture data set with exponentially decaying contribution profiles, Chemom. Intell. Lab. Syst. 37 (1997) 241–254.
[27] P. Stilbs, K. Paulsen, Global least-squares analysis of large, correlated spectral data sets and application to chemical kinetics and time-resolved fluorescence, Rev. Sci. Instrum. 67 (1996) 4380–4386.

[28] M. Nilsson, G.A. Morris, Speedy component resolution: an improved tool for processing diffusion-ordered spectroscopy data, Anal. Chem. 80 (2008) 3777–3782.
[29] K. Takegoshi, K. Ogura, K. Hikichi, A perfect spin echo in a weakly homonuclear *J*-coupled two spin-system, J. Magn. Reson. 84 (1989) 611–615.
[30] P.C.M. van Zijl, C.T.W. Moonen, M. von Kienlin, Homonuclear J refocusing in echo spectroscopy, J. Magn. Reson. 89 (1990) 28–40.
[31] A.M. Torres, G. Zheng, W.S. Price, *J*-compensated PGSE: an improved NMR diffusion experiment with fewer phase distortions, Magn. Reson. Chem. 48 (2010) 129–133.
[32] K.I. Momot, P.W. Kuchel, B.E. Chapman, Acquisition of pure-phase diffusion spectra using oscillating-gradient spin echo, J. Magn. Reson. 176 (2005) 151–159.
[33] M.J. Hubley, T.S. Moerland, Application of homonuclear decoupling to measures of diffusion in biological 31P spin echo spectra, NMR Biomed. 8 (1995) 113–117.
[34] A.M. Torres, R.D. Cruz, W.S. Price, Removal of *J*-coupling peak distortion in PGSE experiments, J. Magn. Reson. 193 (2008) 311–316.
[35] M. Nilsson, G.A. Morris, Improving pulse sequences for 3D DOSY: convection compensation, J. Magn. Reson. 177 (2005) 203–211.
[36] A.C. Wang, A. Bax, Minimizing the effects of radio-frequency heating in multidimensional NMR experiments, J. Biomol. NMR 3 (1993) 715–720.
[37] S.J. Gibbs, C.S. Johnson, A PFG NMR experiment for accurate diffusion and flow studies in the presence of eddy currents, J. Magn. Reson. 93 (1991) 395–402.
[38] M. Liu, J.K. Nicholson, J.C. Lindon, High-resolution diffusion and relaxation edited one-and two-dimensional ^{1}H NMR spectroscopy of biological fluids, Anal. Chem. 68 (1996) 3370–3376.
[39] W.H. Otto, C.K. Larive, Improved spin-echo-edited NMR diffusion measurements, J. Magn. Reson. 153 (2001) 273–276.
[40] J.-M. Böhlen, I. Burghardt, M. Rey, G. Bodenhausen, Frequency-modulated "Chirp" pulses for broadband inversion recovery in magnetic resonance, J. Magn. Reson. 90 (1990) 183–191.
[41] G. Mackin, A.J. Shaka, Phase-sensitive two-dimensional HMQC and HMQC-TOCSY spectra obtained using double pulsed-field-gradient spin echoes, J. Magn. Reson., Ser A 118 (1996) 247–255.
[42] N. Murali, A. Kumar, Coherence transfer via longitudinal spin order generalized pulse pair filtering for pure phase two-dimensional NMR spectroscopy, Chem. Phys. Lett. 137 (1987) 324–329.
[43] P.J. Bowyer, A.G. Swanson, G.A. Morris, Analyzing and correcting spectrometer temperature sensitivity, J. Magn. Reson. 152 (2001) 234–246.
[44] F. Brandl, F. Kastner, R.M. Gschwind, T. Blunk, J. Teßmar, A. Göpferich, Hydrogel-based drug delivery systems: comparison of drug diffusivity and release kinetics, J. Controlled Release 142 (2010) 221–228.
[45] C. Buckley, K.G. Hollingsworth, A.J. Sederman, D.J. Holland, M.L. Johns, L.F. Gladden, Applications of fast diffusion measurement using Difftrain, J. Magn. Reson. 161 (2003) 112–117.
[46] M. Nilsson, M. Khajeh, A. Botana, M.A. Bernstein, G.A. Morris, Diffusion NMR and trilinear analysis in the study of reaction kinetics, Chem. Commun. (2009) 1252–1254.
[47] M. Khajeh, A. Botana, M.A. Bernstein, M. Nilsson, G.A. Morris, Reaction kinetics studied using diffusion-ordered spectroscopy and multiway chemometrics, Anal. Chem. 82 (2010) 2102–2108.